Polarization-Modulated Bent-Core Liquid Crystal Thin Films without Layer Undulation

Cuiyu Zhang,[1] Min Gao,[1] R. R. Ribeiro de Almeida,[1,4] Wolfgang Weissflog,[2]
Oleg D. Lavrentovich,[1,3] and Antal Jákli[1,3,*]

[1]*Chemical Physics Interdisciplinary Program and Advanced Materials and Liquid Crystal Institute, Kent State University, Kent, Ohio 44242, USA*

[2]*Martin Luther University Halle-Wittenberg, Department of Chemistry, Physical Chemistry, von-Danckelmann-Platz 4, 06120 Halle, Germany*

[3]*Department of Physics, Kent State University, Kent, Ohio 44242, USA*

[4]*Department of Physics, Federal University of Technology, Apucarana, PR 86812-460, Brazil*

(Received 17 January 2019; published 5 April 2019)

Spatial confinement is known to affect molecular organizations of soft matter. We present an important manifestation of this statement for thin films of bent-core smectic liquid crystals. Prior freeze-fracture transmission electron microscopy (FFTEM) studies carried out on nitro-substituted bent-core mesogens (n-OPIMB-NO_2) revealed an undulated smectic layer structure with an undulation periodicity of ~8 nm. We report cryogenic TEM measurements on ~100 nm thick 8-OPIMB-NO_2 films. In contrast to FFTEM results, our studies show only density modulation with periodicity $b = 16.2$ nm, and no smectic layer undulation. We show that the discrepancy between the FFTEM and cryogenic transmission electron microscopy (cryo-TEM) results can be attributed to the different sample thicknesses used in the experiments. FFTEM monitors cracked surfaces of a relatively thick (5–10 μm) frozen sample, whereas cryo-TEM visualizes the volume of a thin (0.1 μm) film that was quenched from its partially fluid phase. These results have importance in possible photovoltaics and organic electronics applications where submicron thin films are used.

DOI: 10.1103/PhysRevLett.122.137801

Nanostructures of thermotropic liquid crystals (LCs) in bulk are usually studied by small-angle x-ray scattering (SAXS) or freeze-fracture transmission electron microscopy (FFTEM) techniques. SAXS reveals electron density variation of bulk samples in the range of about 1 to 100 nm, while FFTEM images greater than 2 nm reveal surface modulations of replicas made on cracked bulk samples. Recently it was shown that cryogenic transmission electron microscopy (cryo-TEM) can also provide useful and unique nanoscale information even of single compound LCs [1–4]. Cryo-TEM is imaging lateral electron density modulations with about 0.5 nm resolution in films up to about a hundred nanometer thickness without the need of replication; therefore, it monitors the nanostructure of thin films. This is significant since there is an increasing number of applications where liquid crystals are in thin film forms, such as in photovoltaic [5] and organic electronics [6] applications. For example, layer undulations may not be compatible with smooth surfaces, resulting in considerably different nanostructures in thin films than in bulk samples. Consequently, it is vital to compare nanostructures in different conditions, such as those monitored by FFTEM and cryo-TEM.

The polarization-modulated tilted smectic phase of bent-core liquid crystals [7] (formerly called the $B7$ [8,9] phase [10]) has an extremely interesting nanostructure. In bulk these materials form peculiar micrometer scale helical patterns and slender freely suspended filaments [11–16]. SAXS studies revealed their complex 2D scattering profiles [8,10,17] [see Fig. 1(a)] that could be well indexed by a monoclinic 2D unit cell with lattice parameters $a \sim 3$–5 nm and $b \sim 8$–20 nm. FFTEM studies found that the periodicity b is due to layer undulation [Fig. 1(c)], which forms to avoid density modulation related to ferroelectric polarization splay and the tilted director structure [Fig. 1(b))] [10,18,19]. Later it was proposed that for some of these materials the layer undulation is so strong that the layers break into small ribbons [see Fig. 1(d)], which means that they can be considered as a columnar (originally known as $B1$ [20]) phase [17]. While in the undulated smectic structures the layers are continuous through the polarization splay defects, in the columnar phase the layers have alternating stepwise half layer thickness displacements [21]. Undulations and the stepwise displacements are not likely to form adjacent to flat surfaces; therefore it is interesting to study their structures in thin films.

Recently SAXS and cryo-TEM studies of three nitro-substituted (n-OPIMB-NO_2, $n = 7$, 9, and 16) bent-core LCs were reported [22]. While SAXS studies showed two periodicities between $a_X \sim 3.4$–4.7 nm and $b_X \sim 9$–16 nm (subscript X refers to data measured by x ray), cryo-TEM images did not show the layer spacing a but revealed strong transmitted electron intensity modulation with periodicity $b_T \sim b_X - 1$ nm, where subscript T means it is measured

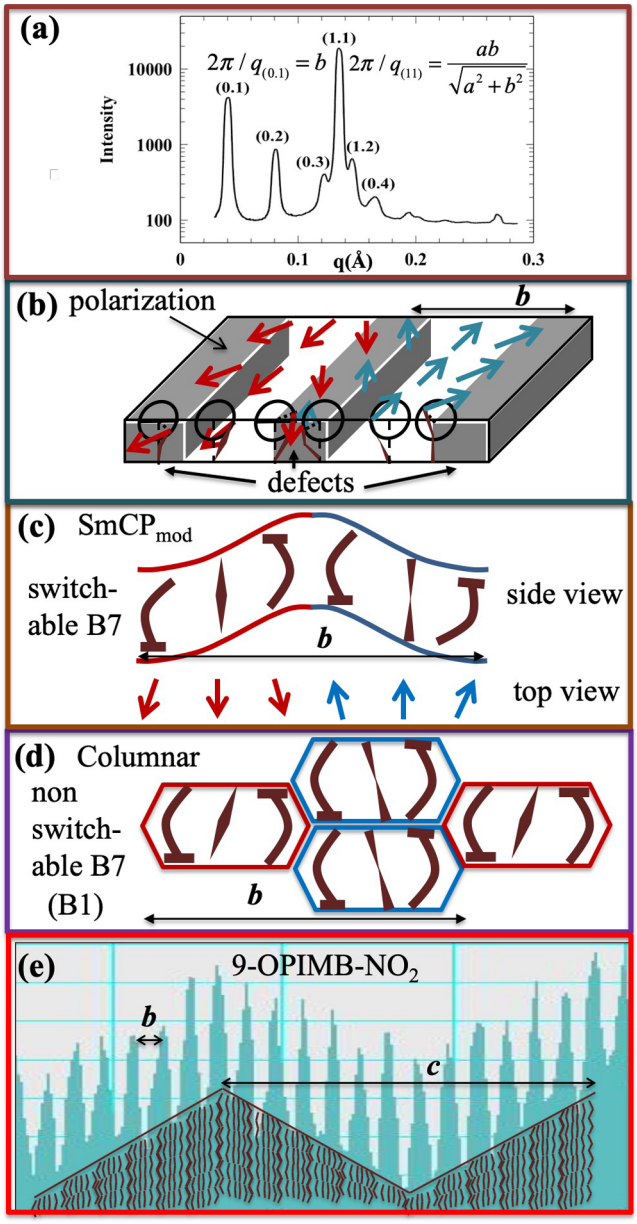

FIG. 1. Summary of the main structural features of the prototype $B7$ materials. (a) Typical q dependence of SAXS intensity at 150 °C. (b) Illustration of the polarization splay and the resulting appearance of periodic defects with lower mass density. (c) Schematics of the undulated layer structure without defects. (d) Columnar structure where the layer undulation is replaced by stepwise displacement of the layers. (e) Transmitted electron density profile observed on 9-OPIMB-NO_2 at 130 °C with overlaid proposed molecular arrangements.

by TEM. Strangely, the intensity variation was much larger than what a layer undulation model could explain. Additionally, an intensity modulation with a period $c \sim$ 100–200 nm was also observed [Fig. 1(e)]. These observations were consistent with a $B1$-type model where the surface of conformal columns alternates being parallel to two different low-order faces of the lattice as illustrated in the overlaid sketch in Fig. 1(e), although it could not explain the large intensity modulation with periodicity b_T.

In this paper we describe cryo-TEM studies of 2-nitro-1,3-phenylenebis[4-(4-octyloxyphenyliminomethyl) benzoate] (8-OPIMB-NO_2) that has been extensively studied in bulk form [10,11,16,17,21,23–25]. In contrast to the prior observations on the $n = 7$, 9, and 16 homologs described above, here both $a_T = a_X$ and $b_T = b_X$ modulations were found. We also show that in 0.1 μm thin film the density modulation caused by the polarization splay domains [see Fig. 1(b)] is not converted to either layer undulations [Fig. 1(c)] or stepwise layer displacements [Fig. 1(d)] that were observed by the Boulder group using FFTEM.

The molecular structure of 8-OPIMB-NO_2 is shown in Fig. 2(a). The extended length of the molecule is 4.7 nm. Prior polarized optical microscopy studies of 8-PIMP-NO_2 revealed formation of typical $B7$-type helical superstructures starting at 177 °C and above the crystal transition at 116 °C [8].

Our cryo-TEM studies were carried out with a FEI Tecnai F20 microscope as described in the Methods section of the Supplemental Material (SM) [26]. Our 8-PIMP-NO_2 films of 70–100 nm thicknesses were quenched from 150 °C. At this temperature prior SAXS studies [10,17] found electron density modulations with 3.6 and 8 to 9 nm periodicities that they make an angle $\gamma = 81°$ with each other and was also concluded that this material has a columnar ($B1$)-type nanostructure, as illustrated in Fig. 1(d) [17,21].

Representative cryo-TEM textures quenched from 150 °C are seen in Figs. 2(b) and 3(a) and Fig. S-1 of the SM [26]. Figure 2(b) shows a cryo-TEM image of an area, with stripes of about 3.6 nm periodicity, that corresponds to the smectic layer spacing, as found by prior SAXS studies [10]. Notably, in the entire area we cannot see any modulation with $b = 16.2$ nm periodicity. The observations of the stripes with periodicity equal to the layer spacing requires a difference in the electron densities of the aromatic molecular cores and hydrocarbon tails, and that the layers be perpendicular to the substrate, as illustrated in Fig. 2(c) [1]. Otherwise the electron beam passing through the material normal to the substrates would hit both the core and tail areas, thus wiping out any electron density contrast [Fig. 2(d)]. The observation of stripes also excludes the columnar model [17,21], since in the case of stepwise half layer shifts [see Fig. 1(c)] the tail and core areas would overlap and would result in no fringes with the periodicity of the layer spacing. As we discuss in the SM [26] and show in Fig. 2(c), the contrast decreases for sinusoidally undulated layers perpendicular to the substrate with the amplitude of the modulation u, and it becomes smaller than the experimental noise for $u \geq a$ [Fig. 2(d)].

Figure 2(e) shows an expected TEM image when the axis of the $b = 16.2$ nm stripes is parallel to the substrates. In this case the $a = 3.6$ nm stripes should appear undulated

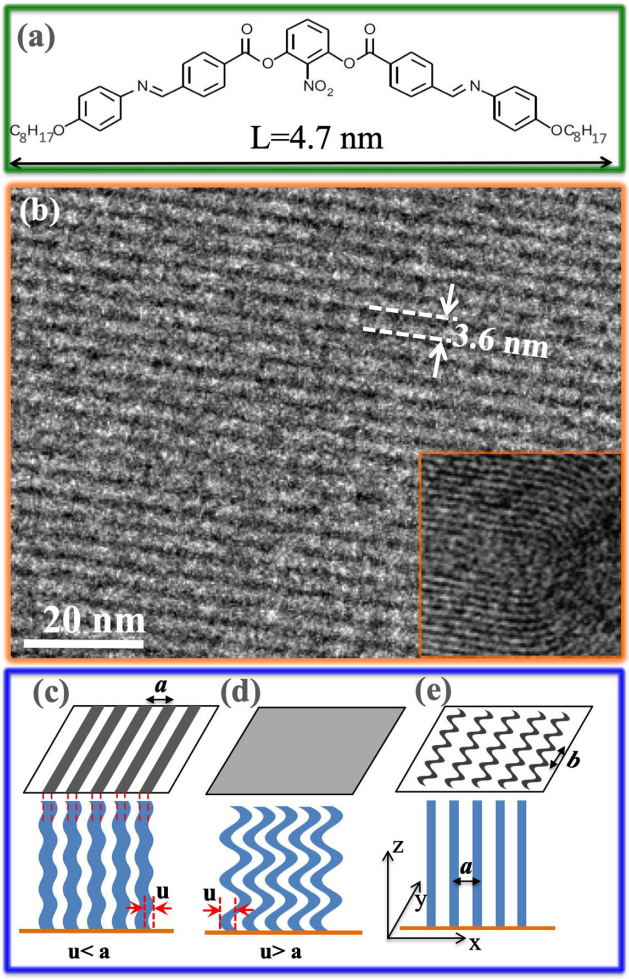

FIG. 2. Molecular structure of the studied 8-OPIMB-NO_2 and the appearance of the $a = 3.6$ nm stripes. (a) Chemical structure of 8-OPIMB-NO_2. (b) Cryo-TEM image of an area with stripes of $a \sim 3.6$ nm periodicity corresponding to smectic layer spacing. In the main panel the smectic layers have uniform direction, whereas the inset at the bottom right shows a defect area where the smectic layers turn around by 180°. (c)–(e) Illustration of expected TEM images in the case of several possible layer undulations—(c) $u < a$, (d) $u > a$, (e) $u = 0$.

with periodicity $b = 16.2$ nm. Careful inspection of hundreds of TEM images could not reveal any undulated pattern. Additional representative cryo-TEM images are shown in Fig. S-1 of the SM [26].

Another significant observation is that, in addition to the fairly straight stripes, we found areas where the layers make a 180° reorientation in the form of a U-turn [inset of Fig. 2(b)] and the layers' normal experiences pure splay, as dictated by the equidistance of smectic layers [27]. This defect structure not only verifies the layered smectic structure but also excludes the possibility of any long-range periodic order within the smectic layers in the plane perpendicular to the disclination axis. In other words, if the $b = 16.2$ nm stripes are present in the structure, they should be aligned horizontally, parallel to the plane of Fig. 2(b).

In contrast to Fig. 2(b), where we see only $a = 3.6$ nm stripes, Fig. 3(a)) shows an area with $b = 16.2$ nm stripes, which is twice that found in bulk by SAXS measurements [10,17,28]. In the main panel the stripes follow a labyrinth-type pattern, whereas the inset on the bottom-right corner shows an area of $b = 16.2$ nm stripes in two coexisting directions. The spatial dependence of the transmitted electron intensity measured across the fringes between A

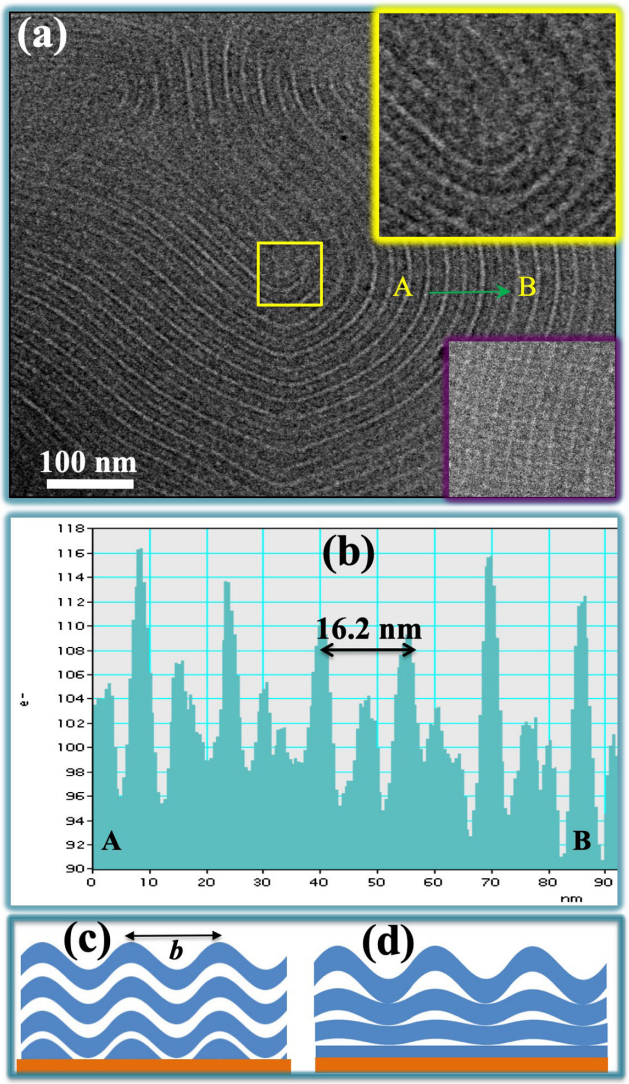

FIG. 3. Summary of cryo-TEM results on an area that shows transmitted electron intensity modulation with periodicity of $b = 16.2$ nm. (a) Cryo-TEM image showing a labyrinth structure of $b = 16.2$ nm stripes. The inset in the right-bottom corner shows an area with crossing $b = 16.2$ nm stripes. (b) The transmitted electron intensity measured along the line from A to B on the main panel of (a). (c),(d) Schematic illustrations of undulating layers along the substrates. (c) Undulation amplitudes are constant normal to the substrate. (d) Undulation amplitude increases normal to the substrate.

and B in the main panel is shown in Fig. 3(b). Although the intensity profile is somewhat noisy (about 30% of the variation $\Delta I_{\max}$), it is clearly seen that there is an additional, weaker maxima between the major peaks. This explains why prior x-ray measurements [10,17,28] have detected periodicity with 8.1 nm. We estimate (see the SM [26]) that the observed intensity modulation would correspond to about a 20 nm variation of film thickness, which is larger than the lateral periodicity b. In view of the physical mechanism of layer undulations proposed by Coleman *et al.* [10], the undulation amplitude should not be larger than $\Delta h_b = \tan\theta(b/2) \approx b/2$. This shows that the observed $b = 16.2$ nm stripes cannot be at least fully due to layer undulations. This actually can be expected since undulated smectic layers running along the flat substrate would be incompatible with the surface, as illustrated in Fig. 3(c). As shown in Fig. 3(c), layers with constant spacing would necessarily lead to a periodic array of defects near the substrate. The appearance of those defects can be avoided only if the layer adjacent to the substrate is not undulated, and the undulation amplitude would increase toward the free surface. In this case, however, the layer spacing would need to change [Fig. 3(d)], which has a large energy penalty. Accordingly, we conclude that the $b = 16.2$ nm stripes represent only density modulations without layer undulations [see Figs. 2(a) and 4(a)], for layers both parallel and perpendicular to the substrates, as evidenced by cryo-TEM results shown in Figs. 2(b) and 3(a), respectively. Such a conclusion also explains the large intensity modulations with $b = 16.2$ nm periodicity observed in films of $n = 7.9$ and 16 homologs of n-PIMB-NO_2 [see Fig. 1(e)].

The thickness h of a film where the undulation is suppressed by the surface can be estimated by balancing the bulk energy of periodic layers' tilts, approximated as $\frac{1}{2}B\int_0^h[\frac{1}{2}(\partial u/\partial x)^2]^2 dz$, and the surface anchoring cost of these tilts that can be written as a quadratic function, $\frac{1}{2}W(\partial u/\partial x)^2$, of the layers' tilt angle, $\partial u/\partial x$. Here B is the layer compression modulus, $u = u_o\cos(2\pi x/b)$, and W is the anchoring strength. The quadratic surface anchoring potential is justified for weakly undulating layers, in which case the sign of the tilt changes periodically along the x axis [29]. Assuming that $u_o \le a/2$ and taking into account that in smectic liquid crystals $W = Ba$ [32], we get $h \ge (16b^2/a) \simeq 0.4\ \mu$m. This value is larger than the thickness of our film and smaller than that used in FFTEM measurements and, thus, appears to explain the differences found between cryo-TEM and FFTEM.

The labyrinth-type pattern of the $b = 16.2$ nm stripes with $\pm 1/2$ disclinations shows the nonpolar character of these stripes (polar stripes could form only integer-strength lines [27]). On the other hand, according to the polarization modulated model of the $B7$ phase [10], each stripe is characterized by a polarization splay, with a nonzero net value. The net polarization in subsequent stripes may alternate as shown in Fig. 4(b), or they can alternate in every other stripe [see Fig. 4(b)]. In both cases the net polarization averages to zero within 16 nm that marks the distance between the larger peaks in Fig. 3(b). That alteration explains the presence of the 1/2 disclination shown in Fig. 3(a). The magnified image of the core of the disclination in the upper inset of Fig. 3(a) shows that the contrast associated with the periodic order practically vanishes within an area of a radius $\sim b$ since at the disclination core the positional order is destroyed [27].

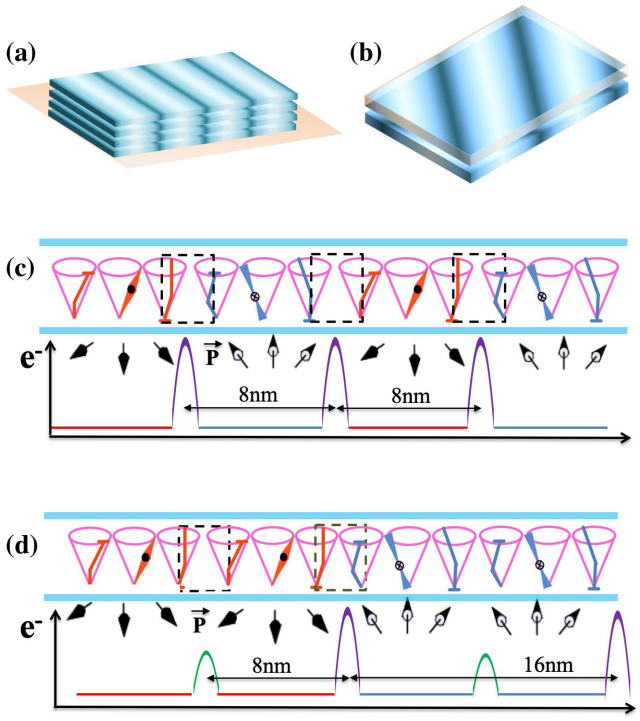

FIG. 4. Proposed models to explain the cryo-TEM images showing area with $b = 16.2$ nm stripes. (a) Schematic illustration of flat layers with electron density modulation corresponding to a local structure of the main panel in (a). (b) Overlapping sheets of flat smectic layers with electron density modulations in different directions corresponding to the inset of Fig. 3(a). (c) Model of director structures with polarization splay modulation that would lead to $b = 16.2$ nm stripes with single intensity modulation (not corresponding to our experimental observation). (d) Model of director structures with polarization splay modulation that would lead to $b = 16.2$ nm stripes with double intensity modulation [corresponding to our experimental observation shown in Fig. 2(b)].

The observation that the $b = 16.2$ nm stripes in the same areas can run in two different directions [see the lower inset of Fig. 3(a) and Fig. S-1(d) of the SM [26]] suggests that layers with electron density modulations in different directions overlap. If there were layer undulations, the overlap would lead to empty volumes, which would be energetically costly. Therefore, we assume in the overlapping areas the layers are flat as schematically illustrated in Fig. 4(b).

To find out which of the polarization splay models of Fig. 4 we are dealing with, we need to analyze the density variations at the domain boundaries. When the polarization directions in the adjacent splay domains alternate, then both the director tilt and molecular bend directions change sign at the domain boundaries, as shown in Fig. 4(c) and Fig. 1(d) of Ref. [10]. That would lead to equal density variations at the domain boundaries, leading to a single periodicity. To explain the double periodicity modulation that we found experimentally, we therefore have to assume that the polarization directions are changing signs only in every other polarization splay domain wall, as illustrated in Fig. 4(d). In that case the density change (and the transmitted electron intensity variation) is smaller when the molecules tilt in the same direction in the neighbor domains, and larger when their tilt directions are opposite at the polarization splay boundary. We note that other local director arrangements, such as doubly tilted SmC_G-type structure of the $B7$ phase [31], could also explain a double periodicity. In that case both the tilt of the molecular planes and the tilt of the director (leaning) would be alternating in adjacent splay domains.

To summarize, the results of our cryo-TEM studies on 8-OPIMB-NO_2 are compatible with the polarization modulation model of Coleman *et al.* [10], but they do not show the secondary layer undulations that were observed by FFTEM measurements in several micrometer thick samples [34]. This shows that the layer undulations appearing in bulk as a consequence of the polarization splay can be suppressed in thin films. Our results therefore show that in submicron thin films the nanostructures of certain liquid crystal phases can be different from those observed in bulk or in films with over a micrometer thickness. We note that size dependent structures are known in other liquid crystals with periodic structures. For example, in chiral liquid crystals a helical pitch is suppressed in films with thicknesses less than the pitch [33], in helical nanofilament or in twist-bend nematic phase the structure is modified at surfaces [3,30]. The unusual feature of the suppression of the layer undulation in the $B7$ phase is the order of magnitude larger thickness range than of the periodicity. The decrease of the density with 8 and 16 nm periodicities would make thin films susceptible for intake of nanoparticles, such as gold, quantum dots or C_{60}. The use of C_{60} may have importance in organic photovoltaics to achieve efficient heterojunctions [35]. The modulated environment influences strongly the electric transport properties, as discussed recently [36].

This work was financially supported by NSF DMR Grant No. 1307674. The TEM data were obtained at the cryo-TEM facility at the Liquid Crystal Institute, Kent State University, supported by the Ohio Research Scholars Program "Research Cluster on Surfaces in Advanced Materials." A. J. and O. D. L. are thankful to Noel Clark for sharing their FFTEM data on the studied material and for the useful discussions.

*Corresponding author.
ajakli@kent.edu

[1] C. Zhang, M. Gao, N. J. Diorio, W. Weissflog, U. Baumeister, S. N. Sprunt, J. T. Gleeson, and A. Jákli, Phys. Rev. Lett. **109**, 107802 (2012).
[2] C. Zhang, B. K. Sadashiva, O. D. Lavrentovich, and A. Jákli, Liq. Cryst. **40**, 1636 (2013).
[3] C. Zhang, N. Diorio, O. D. Lavrentovich, and A. Jákli, Nat. Commun. **5**, 3302 (2014).
[4] M. Gao, Y. K. Kim, C. Zhang, V. Borshch, S. Zhou, H.-S. Park, A. Jákli, O. D. Lavrentovich, M. G. Tamba, G. H. Mehl, D. Studer, B. Zuber, H. Gnägi, and F. Lin, Microsc. Res. Tech. **77**, 754 (2014).
[5] R. A. Callahan, D. C. Coffey, D. Chen, N. A. Clark, G. Rumbles, and D. M. Walba, ACS Appl. Mater. Interfaces **6**, 4823 (2014).
[6] C. M. Keum, S. Liu, A. Al-Shadeedi, V. Kaphle, M. K. Callens, L. Han, K. Neyts, H. Zhao, M. C. Gather, S. D. Bunge, R. J. Twieg, A. Jakli, and B. Lüssem, Sci. Rep. **8**, 699 (2018).
[7] A. Jákli, O. D. Lavrentovich, and J. V. Selinger, Rev. Mod. Phys. **90**, 045004 (2018).
[8] G. Pelzl, S. Diele, A. Jákli, C. H. Lischka, I. Wirth, and W. Weissflog, Liq. Cryst. **26**, 135 (1999).
[9] G. Pelzl, S. Diele, A. Jákli, and W. Weissflog, Liq. Cryst. **33**, 1513 (2006).
[10] D. A. Coleman *et al.*, Science **301**, 1204 (2003).
[11] A. Jákli, D. Krüerke, and G. G. Nair, Phys. Rev. E **67**, 051702 (2003).
[12] A. Nemeş, A. Eremin, R. Stannarius, M. Schulz, H. Nádasi, and W. Weissflog, Phys. Chem. Chem. Phys. **8**, 469 (2006).
[13] A. Eremin, A. Nemeş, R. Stannarius, M. Schultz, H. Nádasi, and W. Weissflog, Phys. Rev. E **71**, 031705 (2005).
[14] R. Stannarius, A. Nemeş, and A. Eremin, Phys. Rev. E **72**, 020702(R) (2005).
[15] A. Eremin, U. Kornek, S. Stern, R. Stannarius, F. Araoka, H. Takezoe, H. Nadasi, W. Weissflog, and A. Jakli, Phys. Rev. Lett. **109**, 017801 (2012).
[16] C. A. Bailey and A. Jákli, Phys. Rev. Lett. **99**, 207801 (2007).
[17] C. L. Folcia, J. Etxebarria, J. Ortega, and M. B. Ros, Phys. Rev. E **72**, 041709 (2005).
[18] N. Vaupotič and M. Čopić, Phys. Rev. E **72**, 031701 (2005).
[19] N. Vaupotič, M. Čopić, E. Gorecka, and D. Pociecha, Phys. Rev. Lett. **98**, 247802 (2007).
[20] G. Pelzl, S. Diele, and W. Weissflog, Adv. Mater. **11**, 707 (1999).
[21] D. A. Coleman, C. D. Jones, M. Nakata, N. A. Clark, D. M. Walba, W. Weissflog, K. Fodor-Csorba, J. Watanabe, V. Novotna, and V. Hamplova, Phys. Rev. E **77**, 021703 (2008).
[22] C. Zhang, S. M. Salili, N. Diorio, W. Weissflog, and A. Jákli, Liq. Cryst. **42**, 1621 (2015).
[23] A. Jákli, C. Lischka, W. Weissflog, G. Pelzl, and A. Saupe, Liq. Cryst. **27**, 1405 (2000).
[24] T. Niori, T. Sekine, J. Watanabe, T. Furukawa, and H. Takezoe, J. Mater. Chem. **6**, 1231 (1996).
[25] L. E. Hough, H. T. Jung, D. Krueerke, M. S. Heberling, M. Nakata, C. D. Jones, D. Chen, D. R. Link, J. A. N. Zasadzinski, G. Heppke, J. P. Rabe, W. Stocker, E. Koerblova, D. M. Walba, M. A. Glaser, and N. A. Clark, Science **325**, 456 (2009).

[26] See Supplemental Material at http://link.aps.org/supplemental/10.1103/PhysRevLett.122.137801 for details of the experimental technique, additional TEM images and calculation of the transmitted electron intensity.
[27] P.-G. de Gennes, *The Physics of Liquid Crystals* (Clarendon Press, Oxford, 1974).
[28] D. A. Coleman, Ph.D. thesis, University of Colorado at Boulder 2003.
[29] T. Ishikawa and O. D. Lavrentovich, Phys. Rev. E **63**, 030501(R) (2001).
[30] M. P. Rosseto, R. R. Ribeiro De Almeida, R. S. Zola, G. Barbero, I. Lelidis, and L. R. Evangelista, J. Mol. Liq. **267**, 266 (2018).
[31] A. Jákli, D. Krüerke, H. Sawade, and G. Heppke, Phys. Rev. Lett. **86**, 5715 (2001).
[32] Z. Li and O. D. Lavrentovich, Phys. Rev. Lett. **73**, 280 (1994).
[33] P. G. de Gennes and J. Prost, *The Physics of Liquid Crystals*, 2nd ed. (Clarendon Press, Oxford, 1993).
[34] N. A. Clark (private communication).
[35] N. S. S. Sam-Shajing Sun, *Organic Photovoltaics: Mechanisms, Materials and Devices*, 1st ed. (Taylor&Francis, Boca Raton, FL, 2005).
[36] R. R. Ribeiro de Almeida, L. R. Evangelista, E. K. Lenzi, R. S. Zola, and A. Jákli, Commun. Nonlinear Sci. Numer. Simul. **70**, 248 (2019).